plotted as a function of $(z-z_0)/a$ for the values $ka=9.0$ and $\delta/2a=0.010$. Even for this rather dissipative guide the improvement is seen to be slight. The asymptotic value of $\lambda(\infty)$ approached as $(z-z_0)/a\to\infty$ is indicated by the arrow at the lower right. In Fig. 2 the ratio of the two components of the excitation $\underline{\Psi}_s(z_0)=\underline{\Theta}_{s,\mu}$ are plotted in the complex plane with $(z-z_0)/a$ as a parameter for the same values of ka and $\delta/2a$. For short lengths of guide the ratio λ is increased by a factor of about 5 if the reflected waves are also optimally adjusted, *i.e.*, $M=2N=4$ modes (two waves propagating in the $+z$ and two in the $-z$ direction) are employed.

The asymptotic value of λ has been computed for two and three modes propagating in the $+z$ direction for several values of ka. There are listed in Table I.

ACKNOWLEDGMENT

The author should like to express his gratitude to his adviser, Prof. N. Marcuvitz. He is also indebted to his colleagues, in particular to Profs. L. B. Felsen and H. Kurss.

Further Considerations on Fabry-Perot Type Resonators*

WILLIAM CULSHAW†, SENIOR MEMBER, IRE

Summary—**An integral equation valid for Fabry-Perot type resonators with reflectors of arbitrary curvature and spacing is derived, and equations for the planar, confocal, and spherical geometries are considered further. A numerical iteration method is used to solve the equations, and the properties of the various solutions for the different kernels are discussed. Results show that the confocal type has the lowest diffraction loss, and that the losses in the planar- and spherical-type geometries are identical, as are the normal mode field distributions over the reflectors, apart from a change in sign of the phase angle. Variational methods are applied to give results for the eigenvalues of the planar geometry with great facility, particularly for cases where the eigenvalues are closely spaced. Some potential uses and the respective merits of the resonators are briefly mentioned.**

I. INTRODUCTION

FREE-SPACE resonators, analogous to the optical Fabry-Perot interferometer, continue to play a dominant role in measurements and physical devices for very short microwaves, and also in the new devices for producing coherent light [1]–[4]. Previous work has discussed the application of this interferometer to millimeter wavelengths [5], [6], an important result being that coupling to such resonators could be effected by a whole series, or grating, of coupling holes over the area of the metallic reflector. Such a method can obviously be applied to reflectors of arbitrary shape [7], and is most useful for very short microwaves where optical methods, such as multilayer dielectric films, are not easy to apply. The planar type of reflector system, due to the absence of mode degeneracy, possesses some advantages in routine measurements of wavelength and dielectric constants [8]. Diffraction losses, though larger for given dimensions than those of the confocal-type resonator [9], can still be made small at the shorter wavelengths, and their effect on measurements reduced. However, for a given wavelength and reflector size, such losses do limit the Q value obtainable, and for some purposes such as filter applications, and threshold conditions in lasers, the confocal type may be preferable. However, the planar geometry, though more critical in adjustment and in the degree of flatness required, readily permits single-mode operation, and potentially gives a larger power output than the confocal.

One of the difficulties in evaluating the quality of these free-space resonators is that of diffraction. This leads to diffraction losses and to phase changes which differ slightly from those corresponding to plane wave propagation. The application of integral equations for the solution of such problems was indicated by Goubau and Schwering in their work on the guided propagation of electromagnetic wave beams [10], [11]. Fox and Li [12] also considered various resonator types, and set up the integral equations using the Huygens-Kirchhoff diffraction theory. Numerical solutions for the eigenvalues and eigenfunctions, or field distribution, were obtained by computing the steady state reached after a large number of bounces between the reflectors. Boyd and Gordon [13] also considered the confocal type resonator in some detail. This arrangement is somewhat unique

* Received January 22, 1962; revised manuscript received May 14, 1962.

† Microwave Physics Laboratory, General Telephone and Electronics Laboratories, Incorporated, Palo Alto, Calif

in that the corresponding integral equation can be solved in closed form, the eigenvalues and eigenfunctions being expressible in terms of the radial and angular wave functions in prolate spheroidal coordinates. It is found in all cases that such resonators possess a set of normal modes corresponding to the eigenvalues and eigenfunctions of the appropriate integral equation. For rectangular geometry such modes may be designated as TEM_{mnq}, as in waveguide terminology. The eigenvalue of a given mode determines the attenuation and phase change occurring per transit due to diffraction.

We present here some further considerations on the application of integral equations to such resonators. The integral equation for a general type of free-space resonator with spherical reflectors is derived, from which the appropriate equations for planar, confocal and spherical geometries may be deduced. The properties of the kernels involved in the integral equations are discussed, and numerical solutions are derived by a numerical iteration method, and by a variational method. Previous work [7] on a focused spherical resonator is extended, and interesting relations between the fields and eigenvalues of the planar and spherical geometries are made evident.

II. Integral Equations for Free-Space Resonators

The integral equations for the field distribution over the reflectors were derived for the planar and confocal geometries [12], [13]. Here these equations and similar ones for other geometries will be obtained by the Fourier transform method. Such methods can be used to consider the vector nature of the problem [14] and are also instructive. However, the present discussion will be limited to a scalar solution, since for laser applications the apertures used will be large in relation to the wavelength.

Consider the planar Fabry-Perot resonator with the arrangement shown in Fig. 1. Assuming a distribution of electric field $E_x = E(x_1, y_1)$ over the plane $z=0$, then the radiated angular spectrum of plane waves is given by

$$g(k_x, k_y) = 1/2\pi \iint E(x_1, y_1) e^{j(k_x x_1 + k_y y_1)} dx_1 dy_1, \quad (1)$$

and the field at the position x, y, d becomes

$$E(x, y, d) = 1/2\pi \iint g(k_x, k_y) e^{-j(k_x x_1 + k_y y_1 + k_z d)} dk_x dk_y. \quad (2)$$

Here k_x, k_y, k_z are the rectangular components of the propagation vector $\mathbf{k}$ of magnitude $2\pi/\lambda$, the discussion being limited to rectangular geometry. Substituting (1) into (2) and integrating over the variables k_x, k_y, the relation between the electric fields at $z=0$ and $z=d$ is thus determined by the integral equation [12]

$$\kappa E(x, y) = \frac{je^{-jkd}}{\lambda d} \int_{-b}^{b} \int_{-a}^{a} E(x_1, y_1) e^{-jk[(x_1-x)^2 + (y_1-y)^2]/2d} dx_1 dy_1, \quad (3)$$

where a and b are the dimensions of the reflectors, and d is the spacing between them. This form utilizes the relation between the steady-state fields given by

$$E(x, y, d) = \kappa E(x_1, y_1) \quad (4)$$

where κ is a constant, or eigenvalue, and represents the attenuation and phase change per transit between the reflectors. The derivation of this and other equations to follow assumes that $\lambda/a \ll 1$, or the reflector dimensions are large compared with the wavelength, and also that

$$[(k_x^2 + k_y^2)/2k][(x^2 + y^2)/2d] \ll 2\pi \quad (5)$$

which reduces to the relation $a^2/\lambda d \ll d^2/a^2$.

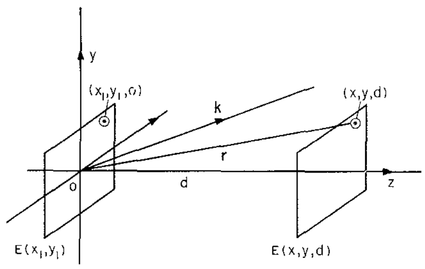

Fig. 1—Planar Fabry-Perot resonator.

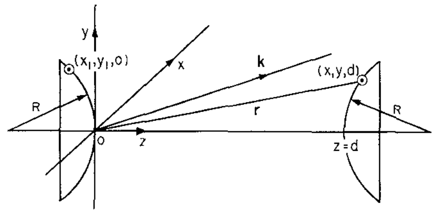

Fig. 2—Convex-type resonator.

Referring to Fig. 2 the integral equation for a resonator with spherical reflectors of radius R separated by a distance d, may now be deduced from (3). Thus on reflection at $z=d$ the field undergoes a total phase change given by the factor $\exp[-jk(x^2+y^2)/R]$. Substituting this result into (4), which gives the relationship between the fields at $z=0$ and $z=d$, and using (3), we obtain after some reduction the general result

$$\kappa E(x, y) = \frac{je^{-jkd}}{\lambda d} \iint E(x_1, y_1) e^{-jkF(x, x_1, y, y_1)/2d} dx_1 dy_1 \quad (6)$$

where

$$F = (1 + d/R)(x_1^2 + y_1^2 + x^2 + y^2) - 2xx_1 - 2yy_1. \quad (7)$$

For $R = \infty$, or planar reflectors, (7) reduces to (3). When $R = -d$, or a confocal reflector system, (6) reduces to the integral equation

$$\kappa E(x, y) = \frac{je^{-jkd}}{\lambda d} \iint E(x_1, y_1) e^{-jk(xx_1 + yy_1)/d} dx_1 dy_1 \quad (8)$$

valid for this geometry. If $R=-d/2$, or a spherical resonator, (7) reduces to

$$kE(x, y) = \frac{je^{-jkd}}{\lambda d} \int\int E(x_1, y_1) e^{jk[(x_1+x)^2+(y_1+y)^2]/2d} dx_1 dy_1 \quad (9)$$

The confocal and spherical resonator types are shown in Figs. 3(a) and 3(b). We shall consider these equations in some detail later; similar equations can be derived for other types of geometry. The discussion is restricted here to the determination of the integral equations for the fields over the reflectors, but by a completely analogous procedure the integral equation for the plane wave spectra radiated by the reflectors could be determined. In any event, the solutions for angular spectra of the modes are given by the Fourier transforms of the eigenfunctions, or field distributions, obtained by solving the integral equations in the field representation.

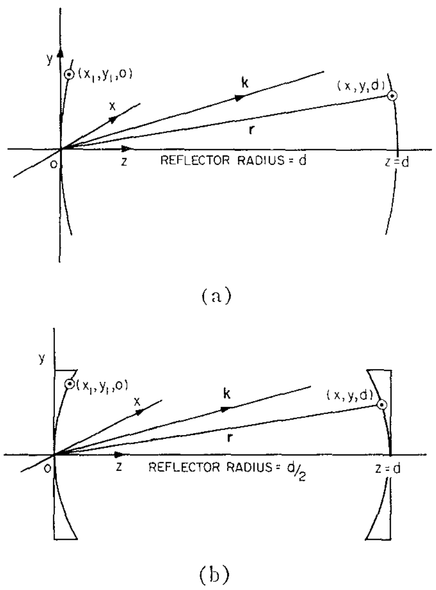

Fig. 3—(a) Confocal resonator. (b) Spherical resonator.

III. Solutions of the Integral Equations

A. General Remarks

A few pertinent remarks on the type of integral equation encountered in the free-space resonator problem are in order at this point. These will be limited to those important in our discussion; more complete treatments are available in the literature [15]–[17]. The equation

$$\psi(x) = \lambda_e \int_a^b K(x, s)\psi(s)ds \quad (10)$$

where the kernel $K(x, s)$ is continuous over the domain $a \leq x \leq b$ and $a \leq s \leq b$, or if the double integral is bounded, *i.e.*,

$$\int_a^b \int_a^b |K^2(x, s)| \, dx \, ds < c_1 \quad (11)$$

where c_1 is a constant, will be termed a linear, homogeneous equation of the Fredholm type. Subject to this condition, the equation will possess solutions $\psi_n(x)$, or eigenfunctions, only for certain discrete values of the parameter λ_e, the eigenvalues. The limits a and b are assumed real and finite, but the parameter λ_e and the functions $\psi_n(x)$, and $K(x, s)$ may be real or complex quantities

A kernel satisfying the equation $K(s, x)=\overline{K}(\bar{x}, s)$, where the bar denotes complex conjugate, is termed Hermitian. The eigenvalues are then all real, and the eigenfunctions are orthogonal in the Hermitian sense, *viz.*,

$$\int_a^b \overline{\psi_m}(\bar{x})\psi_n(x)dx = 0 \qquad m \neq n. \quad (12)$$

They can be normalized and form a complete set of orthonormal functions in terms of which an arbitrary function can be expanded.

If $K(s, x)=K(x, s)$, the kernel is symmetric. The eigenvalues are not real, unless the kernel is real, and the eigenfunctions are only orthogonal in the non-Hermitian sense, *viz.*,

$$\int_a^b \psi_m(x)\psi_n(x)dx = 0 \qquad m \neq n. \quad (13)$$

They do not form a complete orthonormal set of functions.

If the kernel is neither symmetric, nor Hermitian, the equation

$$\phi(x) = \bar{\lambda}_e \int_a^b \overline{K}(\bar{s}, x)\phi(s)ds \quad (14)$$

is called the Hermitian adjoint problem. As indicated, the eigenvalues are the complex conjugates of those of (10). Also if $\psi_n(x)$ and $\phi_m(x)$ are eigenfunctions of (10) and (14) then

$$\int_a^b \overline{\phi_m}(x)\psi_n(x) = 0 \qquad m \neq n, \quad (15)$$

and this relation may be employed to evaluate the coefficients in the expansion of those functions which can be expressed in terms of the eigenfunctions $\psi_n(x)$. The functions ψ_n, and ϕ_m are usually termed biorthogonal functions.

When $K(s, x)=K(x, s)$ the Hermitian adjoint equation (14) reduces to the complex conjugate of (10), and $\phi_n(x)=\overline{\psi}_n(x)$. Various other properties of the solutions may also be derived by utilizing the symmetry of the eigenfunctions. Thus the kernel of (8) for the confocal resonator is symmetric, and the Hermitian adjoint equation for even eigenfunctions reduces again to (8). The conjugate complex eigenfunctions $\psi_{\bar{n}}(x)$ are thus also solutions of (8) and may be combined with $\psi_n(x)$ to give real eigenfunctions and real eigenvalues applicable to this geometry [13]. A similar result is obtained by considering the odd eigenfunctions together with the Hermitian adjoint of (8).

For finite limits a and b, the eigenvalues λ_e of (10) are discrete, but for infinite limits the equation may possess a continuous range of eigenvalues. This corresponds to the diminishing difference between the eigenvalues for our resonators as their lateral dimensions become very large compared with the wavelength, and diffraction losses for the various modes or eigenfunctions become very small. The kernels of the integral equations for the resonators discussed here are continuous and quadratically integrable in the sense of (11). Discrete eigenvalues and corresponding eigenfunctions, or modes of the electric field over the reflectors thus exist, and solutions may be sought by numerical or other methods. A numerical iterative method will be used to determine solutions of the resonator equations. However, when the reflector dimensions become very large in relation to the wavelength, convergence difficulties arise since the eigenvalues become nearly equal in value. For the larger reflector dimensions variational methods can be used with advantage to derive the eigenvalues, using asymptotic waveguide modes or other suitable orthonormal functions for the mode distributions over the reflectors.

B. Solutions by Numerical Integration

In this method the eigenvalues and eigenfunctions are determined approximately as the solutions of the set of n linear equations

$$\psi(x_i) = \lambda_e \sum_{k=1}^{n} D_k K(x_i, x_k)\psi(x_k), \quad i = 1, 2, 3, \cdots, n. \quad (16)$$

Here $K(x_i, x_k) \equiv K_{ik}$ is the value of the kernel when $x = x_i$, and $s = x_k$, and D_k is a weighting coefficient depending on the formula used in numerical integration. It is more expedient to adopt an iteration method of solution [18], using an initial approximation for the eigenfunction, and writing (16) in matrix form. The iteration process will eventually yield the eigenfunction and eigenvalue κ_0 for the dominant mode of the resonator. Convergence is determined by the ratio of κ_1, the next lower eigenvalue, to κ_0, and will become slow for apertures large in relation to the wavelength.

1) Confocal Resonator: Substitute $X = x(k/d)^{1/2}$, $Y = y(k/d)^{1/2}$, and similarly for x_1, y_1, and put $\kappa_e = -j \exp(jkd)\kappa$, where the exponent represents phase changes due to plane-wave propagation between the reflectors, then (8) for the confocal resonator becomes

$$\kappa_e E(X, Y) = 1/2\pi \int_{-Y_0}^{Y_0} \int_{-X_0}^{X_0} E(X_1, Y_1) e^{j(XX_1+YY_1)} dX_1 dY_1 \quad (17)$$

where

$$X_0 = a(k/d)^{1/2}, \qquad Y_0 = b(k/d)^{1/2}.$$

Assume the field is separable, $E(X, Y) = E_1(X)E_2(Y)$, and $\kappa_e = \kappa_1\kappa_2$, then although in general we must assume both $E(X)$ and κ are complex for a complex kernel, in this particular case we can show that with $\kappa_1 = \kappa_c + j\kappa_s$, the equation for $E(X)$ is given by

$$\kappa_c E(X) = (2/\pi)^{1/2} \int_0^{X_0} \cos(XX_1) E(X_1) dX_1 \quad (18)$$

for even modes, and

$$\kappa_s E(X) = (2/\pi)^{1/2} \int_0^{X_0} \sin(XX_1) E(X_1) dX_1 \quad (19)$$

for odd modes. Similar equations hold for $E(Y)$, here we consider only $E(X)$, corresponding to the solution for the infinite strip.

The kernels of (18) and (19) are real and symmetric, and hence Hermitian. The eigenvalues of these equations will all be real, and as already anticipated in Section III-A, the eigenfunctions will also be real. This leads to either real or pure imaginary eigenvalues for the modes, the reflector surface being one of constant phase. Since no mode-dependent phase term appears in the eigenvalues, as also noted by Boyd and Gordon [13], this resonator is highly degenerate, *i.e.*, a large number of modes with the same wavelength will resonate at any given confocal spacing. This may not be serious with an external source as in transmission applications of the resonator, but with internal sources, as in the gas laser, difficulties will arise if laser oscillation in a single mode is desired, since diffraction losses, given by $1 - |\kappa|^2$, are also very small for this resonator and resonances in many higher TEM_{mnq} modes are readily obtained.

Solutions of (18) and (19) can also be found by expanding the kernels in a series of orthogonal functions, but will be derived here by numerical iteration. Consider $X_0 = 1$, and five equally spaced points, $h = (b-a)/n = \frac{1}{4}$, then the matrix expression $[K_{ik}][D_i\delta_{ik}]$ corresponding to (18) is readily determined using, say Simpson's rule [15], and becomes the operator on the column vector $[E]$. Assuming initially that $[E] = \{1, 1, 1, 1, 1\}$, we obtain, after three iterations, the result

$$[K_{ik}][D_i\delta_{ik}][E] = 11.38\{1, 0.99, 0.96, 0.91, 0.85\}. \quad (20)$$

The eigenvalue 11.38 is equal to $12\kappa_1(\pi/2)^{1/2}$, and the maximum of the normalized even mode is at the center of the aperture. This result gives the field distribution over the reflectors and the attenuation per pass for the dominant TEM_{00q} mode of the rectangular confocal resonator for the value of $X_0 = (2\pi/\lambda d)^{1/2}a = 1$. Similar results are obtained for the odd modes from (19).

Table I shows values of κ_c and κ_s for two values of X_0, together with results taken from Boyd and Gordon [13]. The agreement is quite close. Figs. 4(a) and 4(b) show the field distributions over the confocal reflectors as compared with similar results from Fox and Li [12] for circular confocal reflectors. This method of solution is thus relatively simple and accurate for the smaller values of X_0. For larger values of $a^2/\lambda d$, a larger number of intervals must be taken, the convergence becomes slow, and a programmed computer becomes necessary.

TABLE I

VALUES OF κ_c AND κ_s THE LARGEST EIGENVALUES FOR THE EVEN AND ODD MODES OF THE RECTANGULAR CONFOCAL RESONATOR

X_0	$a^2/\lambda d$	κ_c	κ_s	κ
1	0.159	0.7565	0.252j	(ref. [13])
2	0.637	0 9979	0.956j	0.9979 0 9539

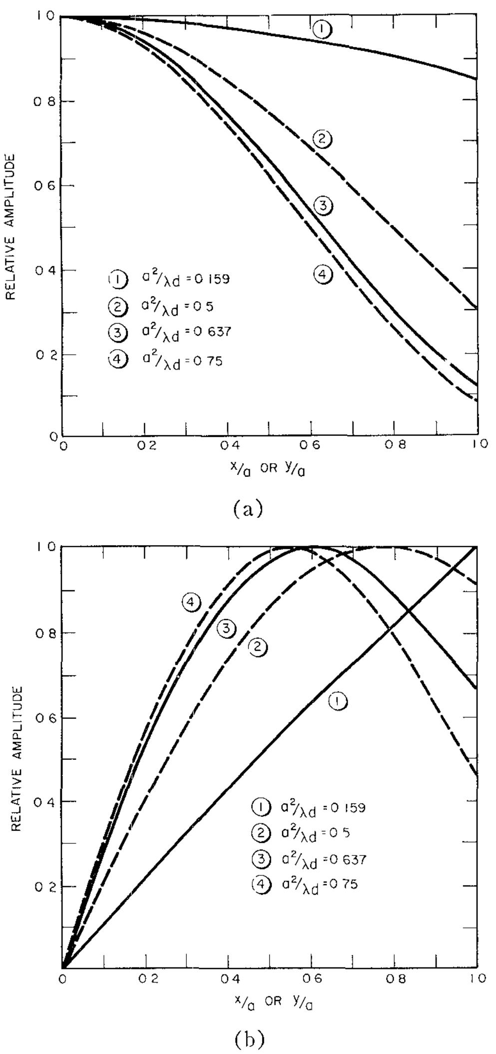

Fig. 4—(a) Amplitude distribution across rectangular confocal reflectors for TEM_{00} mode. Curves 2 and 4, for confocal spherical mirrors after ref. [12], are shown for comparison. (b) Amplitude distribution across rectangular confocal reflectors for TEM_{10} mode. Curves 2 and 4, for confocal spherical mirrors after ref. [12], are shown for comparison.

2) *Planar Resonator*: By a similar reduction (3) for this resonator becomes

$$\kappa E(X) = (1/\pi)^{1/2} \int_{-X_0}^{X_0} E(X_1) e^{-j(X_1 - X)^2} dX_1, \qquad (21)$$

where $X = x(k/2d)^{1/2}$. There is a similar equation for $E(Y)$. The kernel is again complex, symmetric, and non-Hermitian. The fields $E(X)$, and eigenvalues must be assumed complex, and no further reduction as in (18) and (19) is possible. Similar numerical procedures can, however, be applied except that the matrices will now be complex. The appropriate set of linear equations now becomes

$$(\kappa_c + j\kappa_s)[E_r(x_i) + jE_s(x_i)] = (1/\pi)^{1/2} \sum_{k=1}^{n} (K_r + jK_s)[E_r(x_k) + jE_s(x_k)]$$

$$i = 1, 2, 3, \cdots, n \qquad (22)$$

where K_r and K_s are the values of the real and imaginary parts of the kernel for values x_i and x_k. Solutions can now be effected by the numerical iteration method, and will give complex eigenvalues and eigenfunctions for the various modes of the resonator. The complex field distribution means that the reflector is not a constant phase surface for the modes, while the complex eigenvalue shows that phase changes given by $\tan \psi = \kappa_s/\kappa_c$ occur in addition to those corresponding to plane-wave propagation between the reflectors. This means that the modes are no longer degenerate but will resonate at different reflector spacings d. In addition to mode selection in lasers, such modes may be seen by recording the transmitted fringes in a high-quality millimeter wave Fabry-Perot interferometer. Fig. 5 shows a recording made on an improved millimeter wave interferometer [6], the smaller sharp responses to the right of the dominant one are due to other normal modes of the resonator. Actually these mode responses were much larger initially and were reduced by adjustments on the interferometer. The interferometer will resonate at different spacings for the different modes into which the incident field may be resolved, and the transmission through the interferometer can be controlled by adjustments on the reflector alignment and radiator spacings.

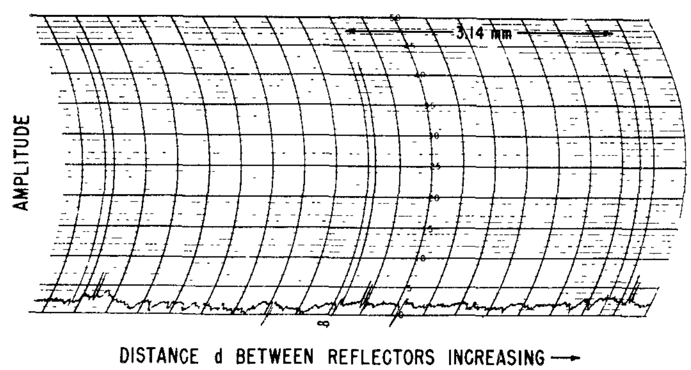

Fig. 5—Millimeter wave interferometer fringes. Small responses to right of main response (sometimes much larger) indicate resonances due to higher-order modes of the planar interferometer. Wavelength 6.28 mm. Brass reflectors 12 in square. Spacing ≃ 10 in.

3) *Spherical or Focused Resonator*: As in Section III-B, 2), (9) for the spherical resonator may be written in the form

$$\kappa E(X) = (1/\pi)^{1/2} \int_{-X_0}^{X_0} E(X_1) e^{j(X + X_1)^2} dX_1, \qquad (23)$$

with a similar equation for $E(Y)$. The eigenvalues and eigenfunctions of this equation are related to those for the planar geometry. Consider the Hermitian adjoint of (21); since the kernel is symmetric, this is equivalent to taking the complex conjugate, *viz.*,

$$\bar{\kappa}\,\overline{E(X)} = (1/\pi)^{1/2}\int \overline{E(X_1)}e^{j(X-X_1)^2}dX_1. \tag{24}$$

For even or odd eigenfunctions (24) may be written as

$$\pm\bar{\kappa}\,\overline{E(X)} = (1/\pi)^{1/2}\int \overline{E(X_1)}e^{j(X+X_1)^2}dX_1, \tag{25}$$

where the minus sign applies to the odd solutions. Comparing (23) and (25), since the kernels are now identical, the solutions for the spherical geometry are determined by the complex conjugates of those for the planar geometry. The eigenvalues for the spherical geometry are the complex conjugates of those for the planar geometry. The attenuation or diffraction loss per transit is thus identical for the two geometries, and since diffraction losses in the planar type are greater than in an equivalent confocal type [13], the spherical resonator cannot have lower losses than a confocal resonator of equivalent dimensions. The modal fields over the spherical reflectors are given by the conjugate complex of those over the planar reflectors, and are thus nondegenerate.

C. Variational Method

The labor involved in the numerical solution of the type of integral equation encountered here is quite large, particularly for large values of the parameter $a^2/\lambda d$. This may not be serious if a computer is used, but in general some variational approach is preferable for such cases. Particularly so since the eigenvalues are all that are usually required, the field distributions having approached asymptotic values very similar to those in metallic waveguides or other orthonormal set of functions. Such asymptotic values can be used in a variational formula for the eigenvalues. Thus, if the kernel $K(x, s)$ in (10) is symmetric, the eigenvalues are given by the stationary values of the ratio [19], [20].

$$\lambda_e = 1/\kappa = \frac{\int_a^b [\psi(x)]^2dx}{\int_a^b\int_a^b K(x, s)\psi(x)\psi(s)dxds}. \tag{26}$$

The stationary values of the ratio occur when $\psi(x)$ is an eigenfunction, and the smallest stationary value, or largest value κ_1, corresponds to the dominant mode $\psi_1(x)$ of the resonator. Other eigenfunctions may then be used to determine κ_2, κ_3, etc., where we have $\kappa_1 \geq \kappa_2 \geq \kappa_3$ and so on. Since the ratio is stationary with respect to the eigenfunctions $\psi_n(x)$, approximations to these functions will give good results for the eigenvalues.

Eq. (26) will now be applied to determine the eigenvalues of (3) applicable to infinite strip plane reflectors, and from Section III-B also applicable to the spherical geometry. Some results for this resonator, derived using the same variational approach, have also been given by Tang [21]. Using the results of Fox and Li [12], and conventional waveguide theory, we represent the eigenfunctions for the even or symmetric modes by

$$\psi(x) = 1/\sqrt{a}\cos n\pi/2\; x/a, \quad n = 1, 3, 5, \text{etc.} \tag{27}$$

Thus from (3) and (26) the eigenvalues for the planar strip geometry are given by

$$\kappa = e^{j(\pi/4)}1/2N^{1/2}\int_{-\sqrt{2N}}^{\sqrt{2N}}\int_{-\sqrt{2N}}^{\sqrt{2N}} \cdot e^{-j(\pi/2)(X-X_1)^2}\cos AX\cos AX_1dXdX_1 \tag{28}$$

where $N=(a^2/\lambda d)$, $A=n\pi/2\sqrt{2N}$, and $x=(2N)^{1/2}x/a$ similarly for X_1, and we have omitted the geometrical phase factor exp $(-jkd)$ in (3). The integration of (28) is laborious but straightforward, and yields the result

$$\kappa_{\text{even}} = \frac{\exp[j(\pi/4+\phi)]}{\sqrt{2}}\left\{-\left(\frac{j}{n\pi}+\frac{n}{8N}\right)\left[F\left(2\sqrt{2N}-\frac{n}{2\sqrt{2N}}\right)+2F\left(\frac{n}{2\sqrt{2N}}\right)-F\left(2\sqrt{2N}+\frac{n}{2\sqrt{2N}}\right)\right]\right.$$
$$\left.+\left[F\left(2\sqrt{2N}+\frac{n}{2\sqrt{2N}}\right)+F\left(2\sqrt{2N}-\frac{n}{2\sqrt{2N}}\right)\right]-1/\pi\sqrt{2/N}\exp[-j(2N\pi+\phi-n\pi/2]\sin(2N\pi-n\pi/2)\right\}, \tag{29}$$

where

$$F(x) = \int_0^x e^{-j(\pi/2)t^2}dt$$

is the Fresnel integral, and $\phi = n^2\pi/16N$.

Eigenvalues for the even modes may be determined for various values of N by substituting $n=1$, 3, 5, etc., into (29). Results for $n=1$ corresponding to the dominant, or lowest loss mode of the resonator, are shown in Table II, together with similar results deduced from Fox and Li [12]. Similar results for $|\kappa_1|$ are also given by Tang [21] for these modes, though the corresponding formula quoted there is incorrect.

We see that the agreement is quite good particularly for the higher values of N where the variational method is expected to yield good results. The eigenvalues for this resonator, as indicated before, are complex, and the additional phase relative to the geometrical term exp $(-jkd)$ contained in (29) yields the frequency separation or positions of resonance for the various modes of the planar type resonator. As shown in Section

TABLE II

EIGENVALUES κ_1 FOR THE DOMINANT MODE OF A PLANAR INFINITE STRIP RESONATOR DEDUCED BY THE VARIATIONAL METHOD

N	κ_1	$\|\kappa_1\|$	$\|\kappa_1\|^*$
$\frac{1}{2}$	0.5919–0.6973j	0.9144	0.911
1	0.6655–0.7045j	0.9692	0.962
2	0.6982–0.7068j	0.9891	0.986
3	0.6994–0.7071j	0.9946	0.992
4	0 7015–0.7071j	0.996	0.995

Values $|\kappa_1|^*$ are values estimated from Fox and Li [12].

TABLE III

EIGENVALUES κ_2 FOR THE LOWEST-ORDER ODD MODE OF A PLANAR INFINITE STRIP RESONATOR DEDUCED BY THE VARIATIONAL METHOD

N	κ_2	$\|\kappa_2\|$	$\|\kappa_2\|^*$
$\frac{1}{2}$	0.2746–0.5666j	0.6297	0.6782
1	0.5440–0.6812j	0.8717	0.8485
2	0.6484–0.7025j	0.9559	0.9327
3	0.6752–0.7053j	0.9763	0.9675
4	0.6858–0.7061j	0.9845	0.9747

Values $|\kappa_2|^*$ are values estimated from Fox and Li [12].

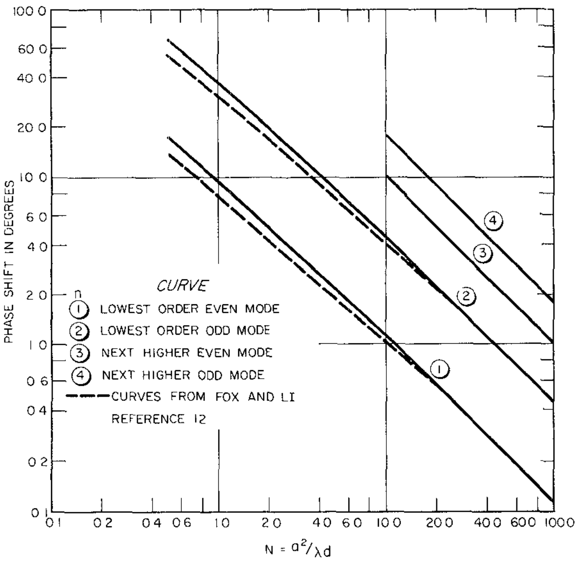

Fig. 6—Variational results on phase shift per transit (leading relative to geometrical phase shift) vs $N=a^2/\lambda d$ for infinite strip reflectors.

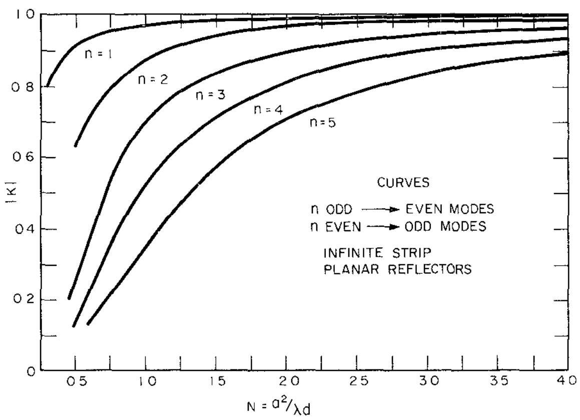

Fig. 7—Moduli of eigenvalues $|\kappa|$ determined by variational method. Curves 1 and 2 lowest-order even and odd modes, respectively.

III-B, 3), such results are also applicable to the spherical resonator. Values of the phase shift per transit deduced from (29) for $n=1$ and various values of N are shown in Fig. 6 where they are also compared with similar results from Fox and Li [12]. Again the variational method gives good results for the higher values of N, and results for the higher modes $n=3$, 5, etc., can also be readily deduced from (29).

Similarly the eigenvalues for the odd modes may be deduced from (26) by substituting the approximate eigenfunctions

$$\psi(x) = 1/\sqrt{a} \sin n\pi/2\; x/a, \qquad n = 2, 4, 6, \text{etc.} \quad (30)$$

The result is that (29) also determines the eigenvalues κ_{odd} for the odd modes when $n=2$, 4, 6, etc. Table III shows the results obtained for κ_2, the first-order odd mode. The agreement is again quite reasonable and would become closer at still larger values of N. The attenuation per transit is higher for this mode particularly at the lower values of N, and the variational method cannot be expected to yield as accurate a result, for a given value of N, as for the dominant mode. Results deduced from (29) are thus more accurate for all modes at the higher values of N, and for the same value of N the error will increase with increase in n. In practice the value of N will be around 20 or more and such limitations to the variational method will not be serious. The accuracy for the lower values of N could in any event be improved if necessary by adopting a Rayleigh-Ritz procedure [20] using a combination of eigenfunctions to represent the field distribution over the reflectors.

Fig. 6 also shows the phase angles deduced for the lower-order odd mode, and Fig. 7 shows the results for $|\kappa|$ for a number of even and odd modes. From (29) the argument of κ approaches the value $\phi_d = n^2\pi/16N$ for large values of N. This corresponds to an effective change δd in the resonator spacing given by

$$\delta d = n^2\lambda/32N, \quad (31)$$

and using values of N commonly encountered in the He-Ne planar reflector type laser, the frequency separation between the dominant and lowest-order odd mode may be deduced. Thus assuming $d=100$ cm, $2a=1$ cm, and $\lambda=1.153\mu$ then $N\simeq 25$. For the modes in question $n=1$, and 2, respectively, and hence from (31) and the equation

$$\delta\nu/\nu = -\delta d/d \quad (32)$$

for the resonator we obtain $\delta\nu=1.12$ Mc. This agrees very well with actually observed beat frequencies in the He-Ne laser [22].

Such a variational method can also be applied to other types of resonators by a suitable choice of an orthonormal set of functions. For the confocal geometry the Hermite polynomials weighted by a Gaussian function are suitable. Such an approach gives the variational result that for the confocal resonator

$$\kappa_n = e^{j(\pi/4)} \frac{1}{\sqrt{2\pi}} \int_{-\sqrt{c}}^{\sqrt{c}} \int_{-\sqrt{c}}^{\sqrt{c}} e^{jxx_1} H_n(x) H_n(x_1) \cdot e^{-x^2/2} e^{-x_1^2/2} dx dx_1 \tag{33}$$

where H_n are Hermite polynomials, and $c = \sqrt{2\pi N}$. This equation may be separated again into two equations for the even and odd modes, and the eigenvalues are either real or pure imaginary quantities. Direct integration of (33) for finite limits $\sqrt{c}$ appears difficult. For infinite limits $|\kappa_0| = 1$ as it should. However, when $\sqrt{2\pi N}$ is large, the difference between the results for finite and infinite limits becomes very small, due to the effect of the Gaussian factors, and it can be surmised, as is already known [13], that the confocal has very low losses for nominal values of N.

IV. Conclusions

Equations analogous to (6) could be used to study the precision to which planar reflectors should be normal to the axis, or to consider the effects of variations in the radius of curvature of the spherical reflectors used in the confocal or spherical geometries. The numerical iteration method used here is very convenient for the smaller values of N, and for resonators with large loss factors such as a convex type of resonator. Here the convergence is rapid and reduces the number of iterations required to establish the results. The result that the eigenfunctions and eigenvalues of the spherical resonator are the complex conjugates of those for the planar resonator is interesting and potentially of some importance in laser applications as regards the ease of reflector adjustment and absence of mode degeneracy in such spherical resonators.

The confocal-type resonator is highly degenerate since the eigenvalues are either real or pure imaginary, the reflector surface being a constant phase surface for all modes. Hence a large number of TEM_{mnq} modes of the same wavelength, given by the equation [13]

$$4d = (2q + 1 + m + n)\lambda \tag{34}$$

can resonate at the same spacing d. If, in addition, the exciting wavelength can vary, due to say the Doppler broadened line in a He-Ne gas laser, then quite complex distributions of fields over the reflectors are possible due to the presence of many simultaneously oscillating modes [23]. This feature is characteristic of the confocal resonator because diffraction losses in this resonator are orders of magnitude smaller than in an equivalent planar type of resonator [13], and become comparable for all modes at values of N used in the laser. It also follows that the spherical resonator cannot have lower diffraction losses than the equivalent confocal type.

Such normal modes of free-space resonators are readily seen in the He-Ne gas laser, particularly in the planar-type resonator, since the laser oscillation will build up in the mode having the lowest diffraction loss. Various mode patterns can be produced by suitable adjustments on the reflector alignment [23]. They can also be seen in transmission measurements with a millimeter-wave planar resonator [6], since the distribution of the incident field will in general contain normal mode distributions of the resonator, and these will be transmitted with varying efficiency at different resonant spacings d. In the past, such effects have been reduced by suitable adjustments on the interferometer, but some further study of them would be useful. Similar remarks are also applicable to the use of millimeter-wave confocal resonators, where the effects on measurements of mode degeneracy, and nonconfocal spacing need investigation.

The efficacy of variational methods is very great, as evidenced by the results obtained on the planar resonator, when we consider that computations involving some 300 transits between the reflectors were necessary to obtain the results given by Fox and Li [12]. A still larger number of transits would be required for higher values of N, whereas the essential results are contained in a single formula for all modes. The method used becomes more accurate the larger the value of N. The phase of the eigenvalue is also determined directly, and is immediately applicable to mode separation problems, and also to the correction of wavelength measurements made on millimeter-wave interferometers. By choosing a more suitable approximation $\psi(x)$ for the eigenfunction at lower values of N, or by a combination of eigenfunctions as in the Rayleigh-Ritz method [22], the accuracy of the variational approach could be improved considerably. This also applies generally, but for the values of N used in present lasers the relatively simpler method adopted here appears adequate.

References

[1] A. L. Schawlow and C. H. Townes, "Infrared and optical masers," *Phys. Rev.*, vol. 112, pp. 1940–1949; December, 1958.

[2] T. H. Maiman, "Optical and microwave-optical experiments in ruby," *Phys. Rev. Letts.*, vol. 4, pp. 564–566; June, 1960.

[3] A. Javan, W. R. Bennett, Jr., and D. R. Herriott, "Population inversion and continuous optical maser oscillation in a gas discharge containing a He-Ne mixture," *Phys. Rev. Letts.*, vol. 6, pp. 106–110; February, 1961.

[4] D. Marcuse, "Maser oscillation observed from HCN maser at 88.6 kMc," Proc. IRE (*Correspondence*), vol. 49, p. 1706; November, 1961.

[5] W. Culshaw, "Reflectors for a microwave Fabry-Perot interferometer," IRE Trans. on Microwave Theory and Techniques, vol. MTT-7, pp. 221–228; April, 1959.

[6] ——, "High resolution millimeter wave Fabry-Perot interferometer," IRE Trans. on Microwave Theory and Techniques, vol. MTT-8, pp. 182–189; March, 1960.

[7] ——, "Resonators for millimeter and submillimeter wavelengths," IRE Trans. on Microwave Theory and Techniques, vol. MTT-9, pp. 135–144; March, 1961.

[8] ——, and M. V. Anderson, "Measurements of dielectric constants and losses with a millimeter wave Fabry-Perot interferometer," *Proc. Conf. Microwave Measurements Techniques, IEE*, London, Eng.; September, 1961. (To be published.)

[9] P. Connes, "Increase of the product of luminosity and resolving power of interferometers by using a path difference independent of the angle of incidence," *Revue d'Optique*, vol. 35, p. 37; January, 1956.
[10] G. Goubau and F. Schwering, "On the Guided Propagation of Electromagnetic Wave Beams," URSI-IRE Spring Meeting, Washington, D. C.; May, 1960.
[11] —— and ——, "On the guided propagation of electromagnetic wave beams," IRE TRANS. ON ANTENNAS AND PROPAGATION, vol. AP-9, pp. 248–256; May, 1961.
[12] A. G. Fox and T. Li, "Resonant modes in a maser interferometer," *Bell Sys. Tech. J.*, vol. 40, pp. 453–488; March, 1961.
[13] G. F. Boyd and J. P. Gordon, "Confocal multimode resonator for millimeter through optical wavelength masers," *Bell Sys. Tech. J.*, vol. 40, pp. 489–508; March, 1961.
[14] J. A. Stratton, "Electromagnetic Theory," McGraw-Hill Book Co., Inc., New York, N. Y., pp. 349–371; 1941.
[15] F. B. Hildebrand, "Methods of Applied Mathematics," Prentice-Hall Book Co., Inc., Englewood Cliffs, N. J., pp. 381–460; 1952.
[16] P. M. Morse and H. Feshbach, "Methods of Theoretical Physics," McGraw-Hill Book Co., Inc., New York, N. Y., pp. 896–992; 1953.
[17] S. A. Mikhlin, "Integral Equations and their Application to Certain Problems in Mechanics, Mathematical Physics, and Technology," Pergamon Press, London-New York, pp. 3–66; 1957.
[18] F. B. Hildebrand, "Methods of Applied Mathematics," Prentice-Hall Book Co., Inc., Englewood Cliffs, N. J., pp. 68–83; 1952.
[19] *Ibid.*, pp. 494–495.
[20] Morse and Feshbach, *op. cit.*, pp. 1106–1158.
[21] C. L. Tang, "On Diffraction Losses in Laser Interferometers," Research Div., Raytheon Co., Waltham, Mass., Tech. Memo T-320; October 23, 1961.
[22] D. R. Herriott, "Optical properties of a continuous helium neon optical maser," *J. Opt. Soc. of America*, vol. 52, pp. 31–37; January, 1962.
[23] W. W. Rigrod, H. Kogelnik, D. J. Brangaccio, and D. R. Herriott, "Gaseous optical maser with external concave mirrors," *J. Appl. Phys.*, vol. 33, pp. 743–744; February, 1962.

Stepped-Impedance Transformers and Filter Prototypes*

LEO YOUNG†, SENIOR MEMBER, IRE

Summary—Quarter-wave transformers are widely used to obtain an impedance match within a specified tolerance between two lines of different characteristic impedances over a specified frequency band. This paper gives design formulas and extensive tables of designs, most of which were especially derived so that an integrated account could be presented for the first time. Numerous examples are given. Only homogeneous, synchronous transformers and filters are included in this paper, but a short bibliography on related topics is appended.

The theory is also applied to band-pass filters, by showing how to convert quarter-wave transformers into half-wave filter prototypes. The theoretical and numerical results presented are applicable to the design of impedance transformers, direct-coupled cavity filters, short-line low-pass filters, optical antireflection coatings and interference filters, acoustical transformers, branch-guide directional couplers, TEM-mode coupled-transmission-line directional couplers, and other circuits. These applications have been or will be dealt with in separate papers; this paper gives the basic theory and some of the numerical data required for these applications.

I. INTRODUCTION

THE OBJECTIVE of this paper[1] is to extend and consolidate the theory of the quarter-wave transformer, with two applications in mind: the first application is as an impedance-matching device or, literally, transformer; the second is as a prototype circuit, which shall serve as the basis for the design of various filters and directional couplers.

* Received April 9, 1962. This work was sponsored by the U. S. Army Signal Research and Development Laboratory, Fort Monmouth, N. J., under contract No. DA 36-039 SC 87398.
† Stanford Research Institute, Menlo Park, Calif.
[1] A more complete treatment is given in [1], on which this paper is based.

This paper is organized into nine parts, with the following purpose and content:

Section I is introductory. It also discusses applications, and gives a number of definitions.

Sections II and III deal with the performance characteristics of quarter-wave transformers and half-wave filters. In these parts the designer will find what *can* be done, not how to do it.

Sections IV to IX tell *how* to design quarter-wave transformers and half-wave filters. If simple general design formulas were available, solvable by nothing more complicated than a slide-rule, these parts would be much shorter.

Section IV gives exact formulas and numerical solutions for Chebyshev and maximally flat transformers of up to four sections.

Section V gives exact numerical solutions for maximally flat (but not Chebyshev) transformers of up to eight sections.

Section VI gives a first-order theory for Chebyshev and maximally flat transformers of up to eight sections, with explicit formulas and numerical tables. It also gives a general first-order formula, and refers to existing numerical tables published elsewhere which are suitable for up to 39 sections, and for relatively wide (but not narrow) bandwidths.

Section VII presents a modified first-order theory, accurate for larger transformer ratios than can be designed by the (unmodified) first-order theory of Section VI.

Sections VIII and IX apply primarily to prototypes